Phytomedicine 41 (2018) 45–53

Contents lists available at ScienceDirect

Phytomedicine

journal homepage: www.elsevier.com/locate/phymed

Original Article

Kidney protection effects of dihydroquercetin on diabetic nephropathy through suppressing ROS and NLRP3 inflammasome

Ding Tao[a], Wang Shaofei[b], Zhang Xuyao[b], Zai Wenjing[b], Fan Jiajun[b], Chen Wei[b], Bian Qi[a], Luan Jingyun[b], Shen Yilan[a], Zhang Yanda[c], Ju Dianwen[b,*], Mei Xiaobin[a,*]

[a] Department of Nephrology, Changhai Hospital, Second Military Medical University, Shanghai 200433, PR China
[b] Department of Microbiological and Biochemical Pharmacy & Key Lab of Smart Drug Delivery, Ministry of Education, School of Pharmacy, Fudan University, Shanghai 201203, PR China
[c] Department of Cardiology, Changzheng Hospital, Second Military Medical University, Shanghai 200003, PR China

ARTICLE INFO

Keywords:
Diabetic nephropathy
Dihydroquercetin
ROS
NLRP3 inflammasome
Extracellular matrix

ABSTRACT

Background: Diabetic nephropathy (DN), the leading cause of end-stage renal disease, is acknowledged as an independent risk factor for cardiovascular disease, which underlines the urgent need for new medications to DN. Dihydroquercetin (DHQ), an important natural dihydroflavone, exerts significant antioxidant, anti-inflammatory, and antifibrotic properties, but its effects on DN have not been investigated yet.

Purpose: We aimed to explore the kidney protection effects of DHQ on DN rats induced by high-fat diet/streptozotocin *in vivo* and the underlying mechanisms of DHQ on renal cells including HBZY-1 and HK2 exposed to high glucose *in vitro*.

Methods: Major biochemical indexes were measured including urine microalbumin, fasting serum glucose, serum levels of creatinine, total cholesterol and low density lipoprotein cholesterol. Renal histologic sections were stained with hematoxylin-eosin, periodic acid-Schiff and Masson. The cell proliferation was assessed by MTT assay. Reactive oxygen species (ROS) generation was detected by DCFH-DA assay and laser scanning confocal microscope. Expression of all proteins was examined by western-blot.

Results: In high-fat diet/streptozotocin-induced DN rats, DHQ at the dose of 100 mg/kg/day significantly attenuated the increasing urine microalbumin excretion, hyperglycemia and lipid metabolism disorders, and mitigated renal histopathological lesions. In *in vitro* studies, DHQ significantly suppressed cell proliferation and the excessive ROS generation, and alleviated the activation of nucleotide binding and oligomerization domain-like receptor family pyrin domain-containing 3 (NLRP3) inflammasome and the expression of renal fibrosis-associated proteins in renal cells exposed to high glucose.

Conclusion: The results revealed that DHQ possesses kidney protection effects including attenuating urine microalbumin excretion, hyperglycemia and lipid metabolism disorders, and mitigating renal histopathological lesions on DN, and one of the possible renal-protective mechanisms is suppressing ROS and NLRP3 inflammasome.

Introduction

As one of the most important complications of diabetes mellitus, diabetic nephropathy (DN) is the major cause of end-stage renal disease (ESRD) with gradually increased urine microalbumin excretion and glomerulosclerosis, and is acknowledged as an independent risk factor for cardiovascular disease (Si et al., 2014). Despite the exact mechanisms have not been well elucidated, it's known that a variety of factors are involved in the onset and progression of DN including genetic factors, representative glomerular hypertension, hyperfiltration and hyperperfusion of abnormal renal hemodynamics in early stage, and hyperglycemia-induced metabolic disorders (Zheng et al., 2016). Lots of data show that the oxidative stress and chronic low-grade inflammation play fundamental key roles in DN (Elmarakby and Sullivan, 2012). Although with intensive control of glucose, lipids and blood pressure, DN is lack of effective treatments except for kidney replacement

Abbreviations: DN, diabetic nephropathy; ESRD, end-stage renal disease; DHQ, dihydroquercetin; ROS, reactive oxygen species; NLRP3, nucleotide binding and oligomerization domain-like receptor family pyrin domain-containing 3; HFD, high-fat diet; STZ, streptozocin; ELISA, enzyme-linked immunosorbent assay; H&E, hematoxylin-eosin; PAS, periodic acid-Schiff; NG, normal glucose; HG, high glucose; ECM, extracellular matrix; MTT, 3-(4,5-dimethylthiazol-2-yl)-2,5-diphenyltetrazolium bromide

* Corresponding authors.
E-mail addresses: dianwenju@fudan.edu.cn (D. Ju), meixiaobin@smmu.edu.cn (X. Mei).

https://doi.org/10.1016/j.phymed.2018.01.026
Received 8 November 2017; Received in revised form 7 January 2018; Accepted 23 January 2018

therapy when progresses to ESRD with the average incidence rate ranging from 30% to 40% globally in diabetic patients (Lopes, 2009; Vega-Diaz et al., 2015). Therefore, exploring new drugs or treatments is urgent for DN.

Dihydroquercetin (DHQ), also known as taxifolin, is an important dihydroflavone compound commonly found in *Larix sibirica Ledeb. (Pinaceae)* and *Pseudotsuga taxifolia Lamb. & Britton (Pinaceae)* (Yang et al., 2016), It exerts lots of biological effects, including anti-oxidant, anti-inflammatory, anti-tumor, antiviral and prevention of Alzheimer's disease, among others (Weidmann, 2012). It attenuated cerebral ischemia-reperfusion injury by inhibiting the production of oxidase and reactive oxygen species (ROS) (Maksimovich et al., 2014). Studies also proved that DHQ improved capillary microcirculation and antiplatelet aggregation, and reduced the production of lipid-free radicals in a dose-dependent manner (Vladimirov et al., 2009). A recent study of mouse model established by transverse aortic constriction confirmed that DHQ attenuated left ventricular fibrosis and collagen synthesis through abrogating the phosphorylation of Smad2 and Smad2/3 nuclear translocation, and inhibiting excess production of ROS, ERK1/2, JNK1/2 after pressure overload (Guo et al., 2015). DHQ also reduced the cholesterol esterification of hepatocytes, triacylglycerol and phospholipid synthesis, decreased apolipoprotein B secretion and inhibited the microsomal triglyceride synthesis (Casaschi et al., 2004). Recent studies revealed that DHQ showed cardio-protective effects against diabetic cardiomyopathy by inhibiting NADPH oxidase, activating JAK2/STAT3 cascade activation and decreasing angiotensin II production(Sun et al., 2014). However, the effect of DHQ against DN hasn't been explored before and whether DHQ is effective to treat DN is unclear.

In this work, we attempted to explore the kidney protection effects of DHQ on DN rats induced by high-fat diet (HFD)/streptozotocin (STZ) *in vivo* and on renal cells including HBZY-1 and HK2 exposed to high glucose *in vitro*. We particularly investigated the protective effects of DHQ on the urine microalbumin excretion, glucose and lipid metabolisms and renal lesions, and explored the underlying mechanisms of these renal protective effects.

Materials and methods

Materials and reagents

High-fat diet food (40 kJ/kg, 20% fat) was purchased from SLAC Laboratory Animal Co. Ltd. (Shanghai, China). Streptozocin (STZ) was acquired from Sigma (St Louis, MO, USA). Cozaar (Losartan Potassium Tablets) and DHQ (purity > 99%) were obtained from Merck Sharp & Dohme (Hangzhou, China) and the Yuanye company (Shanghai, China) respectively. Labrasol was purchased from Gattefosse (Gennevilliers, France). Urine microalbumin enzyme-linked immunosorbent assay (ELISA) kits were obtained from Jianglaibio Co. Ltd. (Shanghai, China). The relevant assay kits were purchased from Jiancheng Bioengineering Institute (Nanjing, China) for measurement of glucose, creatinine, total cholesterol and low density lipoprotein cholesterol. The primary antibodies used in the *in vitro* study for Western-blot were as follows: anti-Fibronectin and anti-Collagen IV (Abcam, Cambridge, MA, USA); anti-NLRP3 (Epitomics, Burlingame, CA, USA); anti-Cleaved Caspasse-1, anti-IL-1β and anti-β-actin (Cell Signaling Technology, Danvers, MA, USA). The secondary antibodies including peroxidase-conjugated goat anti-rabbit and anti-mouse immunoglobulin G (IgG) were obtained from Jackson ImmunoResearch Laboratory (West Grove, PA, USA).

Animals and model establishment

Male SD rats (4–5 weeks old, 110–150 g) were obtained from the Sipper-BK Laboratory Animal Co. Ltd. (Shanghai, China), and three rats were housed per cage in a specific-pathogen-free-conditioned room (at 25 ± 1 °C) with 55–60% relative humidity under a 12-h light/dark cycle and provided with food and water ad libitum. All animals-involving procedures were conducted in strict accordance with the guidelines and protocols approved by the Animal Ethics Committee of School of Pharmacy at Fudan University. To minimize suffering of rats, surgery was performed under anesthesia with intraperitoneal injection of 10% chloral hydrate. Rats were randomly divided into 2 groups after a week adaption period: (1) control group: 10 rats; (2) High-fat diet group: 63 rats. Rats were fed with high fat diet (40 kJ/kg, 20% fat) in the HFD group and were fed with normal pellet diet (20 kJ/kg, 5% fat) in the control group for 4 weeks, then rats in the HFD group were given a single intraperitoneal dose of 30 mg/kg streptozotocin (STZ) dissolved in ice-cold sodium citrate buffer (0.1 M, pH 4.4) and rats in control group were injected with same volume of sodium citrate buffer. Three days after STZ injection, rats with tail fasting blood glucose level beyond 16.7 mmol/l measured using ACCU-CHEK (Roche, Switzerland) were considered as diabetic and randomly divided into 5 groups with treatment for 12 weeks: (1) DN group; (2) DN + DHQ 25 mg/kg/day group; (3) DN + DHQ 50 mg/kg/day group; (4) DN + DHQ 100 mg/kg/day group; (5) DN + Losartan 20 mg/kg/day group, each group consisted of 10 rats. DHQ was dissolved in Labrasol at 35 °C in ultrasound bath for 30 min *in vivo* study. Body weight and fasting serum glucose were determined every two weeks. At the end of the experimental protocol, urine of 24 h was collected to determine the urine microalbumin, then all rats were weighted and sacrificed under anesthesia, and samples were soon collected including blood and kidney. The renal index (mg/g) was calculated as: renal index = kidney weight (mg)/body weight (g).

Serum and urine biochemical parameters analysis

The levels of urine microalbumin were measured by ELISA according to the manufacturer's instructions. The relevant assay kits were obtained for determining levels of fasting serum glucose by glucose-oxidase/peroxidase method, determining serum levels of creatinine through sarcosine oxidase method, determining serum levels of total cholesterol by GPO-PAP enzymatic method and measuring the serum level of low density lipoprotein cholesterol through two direct methods (Nankar and Doble, 2017).

Tissue collection and renal histopathology

After rats sacrificed, kidneys harvested were sectioned longitudinally and fixed in 4% paraformaldehyde solution for 24 h, then were paraffin-embedded and sectioned at 4 μm. At least 10 randomly selected renal histologic sections in each group were stained with hematoxylin-eosin (H&E) for general morphological analysis, periodic acid-Schiff (PAS) for glomerulosclerosis evaluation, and Masson for collagen deposition and interstitial lesions assessment, respectively. 20 glomeruli randomly selected from each group were quantified in PAS-stained sections using ImageJ software 1.42q (National Institute of Health, Bethesda, MD, USA) to assess the percentage of PAS-positive area in glomerulus which was denoted as mesangial index.

Cell culture

Rat kidney mesangial cells (HBZY-1) and human proximal renal tubular epithelial cells (HK2) were purchased from the Chinese Type Culture Collection (CTCC, Shanghai, China), and were maintained in RPMI-1640 medium (Thermo Scientific HyClone, Beijing, China) supplemented with 100 U/ml of a penicillin/streptomycin mixture (Beyotime, Shanghai, China) and 10% fetal bovine serum (Capricorn Scientific GmbH, Ebsdorfergrund, Germany). The cells were routinely grown in 25-cm^2 cell culture plates (Corning Inc., Corning, NY, USA) at 37 °C in a humidified atmosphere with 5% carbon dioxide. DHQ was freshly dissolved in dimethyl sulphoxide (DMSO) as a stock solution and diluted with RPMI 1640 medium when used (The concentration of

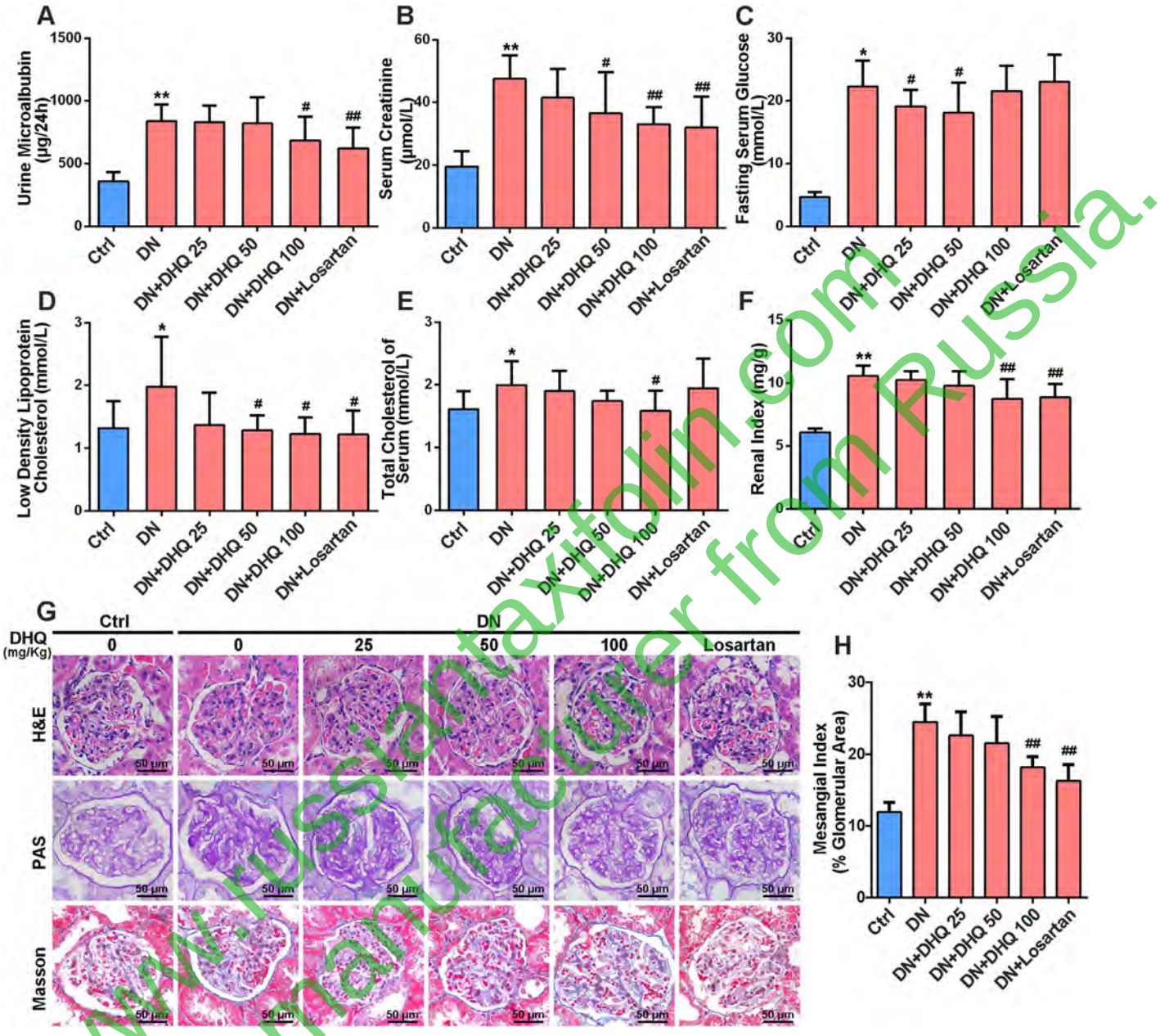

Fig. 1. Effect of DHQ treatment on renal function, glycemic and metabolic change, and renal histopathological fibrosis in HFD/STZ-induced DN rats. (A) Urine microalbumin excretion levels of 24 h. (B) Serum levels of creatinine. (C) Levels of fasting blood glucose. (D) Levels of serum low density lipoprotein cholesterol. (E) Levels of serum total cholesterol. (F) The renal index. (G) Histopathological manifestation of kidney stained with hematoxylin and eosin, periodic acid-Schiff and Masson respectively (Origin magnification: ×400. Scale bar = 50 μm). (H) Glomerular mesangial matrix expansion quantified from PAS staining. Data were presented as the mean ± S.D. ($^{*}P < 0.05$, $^{**}P < 0.01$ versus control group. $^{\#}P < 0.05$, $^{\#\#}P < 0.01$ versus DN group).

DMSO was equal in all groups of 0.1%).

Cell proliferation assay

Cell proliferation was assessed using the 3-(4,5-dimethylthiazol-2-yl)-2,5-diphenyltetrazolium bromide (MTT) assay. Cells in monolayer culture growing to subconfluence were washed twice with phosphate-buffered saline (PBS), and were then re-suspended in culture medium, counted, and seeded in 100 μl media at 4000 cells/well in 96-well microliter plates with 6 parallel wells in each group, and then exposed to normal glucose (5 mmol/l) or high glucose (30 mmol/l) with DHQ added to each well at a final concentration of 10 μM, 20 μM, 40 μM and 80 μM, respectively. The plates were further incubated at 37 °C for 48 h and 72 h in a CO_2 incubator, respectively. The cells were incubated with MTT solution (0.5 mg/ml) for 4 h at 37 °C. Then, 100 μl DMSO was added to each well following the MTT solution discarded. Evenly shaking the 96-well plates resulted in complete dissolution of formazan, and the optical density (OD) was measured at an absorbance wavelength of 570 nm.

Detection of intracellular ROS generation and mitochondrial ROS production

Cells were seeded in 100 μl media at 4000 cells/well in 96-well black plates with 6 parallel wells in each group, and then exposed to normal glucose (5 mmol/l) or high glucose (30 mmol/l) with DHQ added to each well at a final concentration of 5 μM, 10 μM, 20 μM, respectively. The plates were further incubated at 37 °C for 24 h. Cells then were loaded with DCFH-DA, a fluorescent probe for ROS (Beyotime, China) at 10 μM in all wells. After further culture for 20 min

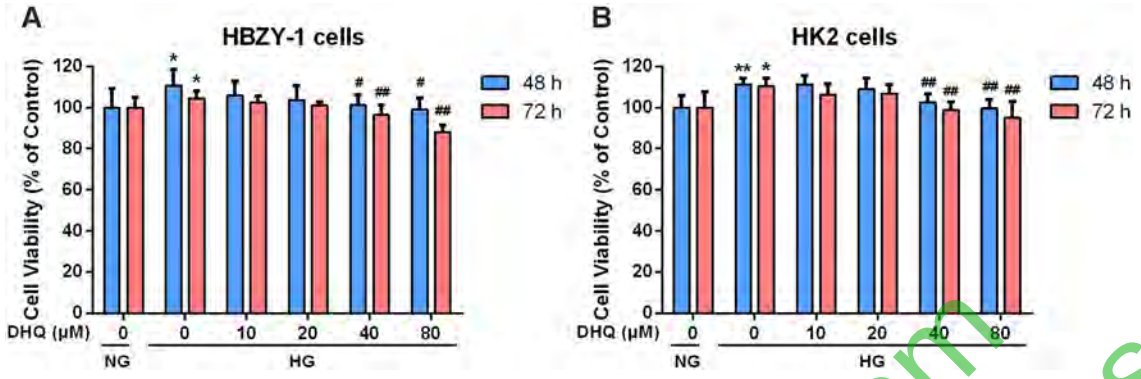

Fig. 2. Effect of DHQ on the proliferation of HBZY-1 and HK2 cells induced by high glucose. (A) The proliferation of rat kidney mesangial cells (HBZY-1) induced by high glucose (30 mM) at 48 h and 72 h. (B) The proliferation of human proximal renal tubular epithelial cells (HK2) induced by high glucose (30 mM) at 48 h and 72 h. $N = 6$ per group ($^{*}P < 0.05$, $^{**}P < 0.01$ versus the NG group. $^{\#}P < 0.05$, $^{\#\#}P < 0.01$ versus the HG group).

in dark, the cells were detected by fluorescence spectrophotometer. To investigate the mitochondrial ROS generation, cells were plated on glasscover-slips in 35 mm diameter dishes at a density of 1×10^5 cells/ml. After adhesion, cells then exposed to normal glucose (5 mmol/l) or high glucose (30 mmol/l) and were treated simultaneously with or without 20 μM DHQ for 24 h. Meanwhile, the mannitol group without DHQ was set to exclude osmotic impact (5 mmol/l glucose + 25 mmol/l mannitol). Then, cells were stained with MitoSOX dye (red) and Hoechst 33342 (blue) at 37 °C for 30 min following the manufacturer's instruction. All the procedures were done in the dark and the samples were observed by a laser scanning confocal microscope.

Western blotting

Cells were seeded in 2 ml media at 8×10^4 cells/well in 6-well plates with 3 parallel wells in each group. After adhesion, cells then exposed to normal glucose (5 mmol/l) or high glucose (30 mmol/l) with DHQ added to each well at a final concentration of 5 μM, 10 μM, 20 μM respectively for 72 h. Meanwhile, the mannitol group without DHQ was set to exclude osmotic impact (5 mmol/l glucose + 25 mmol/l mannitol). Then cells were harvested using Radio Immunoprecipitation Assay (RIPA) Lysis Buffer (Beyotime, China). Cell lysates (20 μg) were electrophoresed on polyacrylamide gels and transferred to PVDF membranes (Millipore, Bedford, MA, USA). The membranes were blocked with TBS containing 3% bovine serum albumin and 0.1% Tween-20 (Sigma-Aldrich), and afterward incubated with the primary antibody and secondary antibodies and then analyzed using an enhanced chemiluminescent detection kit (Pierce, Rockford, IL, USA). Semi-quantitative Western-blot analysis was conducted through measuring the Optical Densitometry in three independent experiments using ImageJ software.

Statistical analysis

Statistics analysis was carried out with GraphPad Prism 6 (GraphPad Software Inc., San Diego, CA, USA). The results from at least three independent experiments were expressed as mean ± standard deviations (S.D). Comparisons between different groups were performed using Student's t test (two-tailed) or one-way ANOVA. A p value < 0.05 was considered statistically significant.

Results

Effect of DHQ treatment on the urine microalbumin excretion, serum level of creatinine, hyperglycemia and lipid metabolism disorders, and renal histopathological lesions in HFD/STZ -induced DN rats.

The urine microalbumin excretion of 24 h reflecting the renal injuries and serum levels of creatinine reflecting the renal functions were measured at the end of DHQ administration for 12 weeks in HFD/STZ-induced DN rats. Urine microalbumin and serum creatinine distinctly increased in DN group compared with the control group, and decreased in the groups administrated with DHQ in a dose-dependent manner. Especially, the levels of urine microalbumin in the group with DHQ 100 mg/kg/day was significantly lower than those in the DN group ($P < 0.05$) (Fig. 1A). The serum levels of creatinine were significantly lower in the groups with DHQ 50 mg/kg/day and DHQ 100 mg/kg/day than those in the DN group ($P < 0.05$, $P < 0.01$ respectively) (Fig. 1B). Fasting serum glucose was determined to assess the effect of DHQ on abnormal glucose metabolism. The increased levels of fasting serum glucose in the DN group compared with the control group ($P < 0.05$) were significantly decreased in the DN rats treated with DHQ 25 mg/kg/day and DHQ 50 mg/kg/day ($P < 0.05$, $P < 0.05$ respectively), but the glucose levels were not altered in the groups with DHQ 100 mg/kg/day compared with the DN group (Fig. 1C). The elevated levels of low density lipoprotein cholesterol and total cholesterol in the DN group compared with the control group decreased with administration with DHQ. Especially, levels of low density lipoprotein cholesterol of the group with DHQ 50 mg/kg/day and DHQ 100 mg/kg/day were signficantly lower than those of the DN group ($P < 0.05$, $P < 0.05$) (Fig. 1D), and the levels of total cholesterol of the group with DHQ 100 mg/kg/day were signficantly lower than the DN group ($P < 0.05$), and there was no difference between the groups with DHQ less than 100 mg/kg/day and the DN group (Fig. 1E). The renal index increased significantly in the DN group compared with the control group and overtly decreased in the DN + DHQ 100 mg/kg/day group compared with the DN group ($P < 0.01$) (Fig. 1F).

Renal histologic sections were stained with H&E, PAS and Masson respectively. Without DHQ, rats in the DN group experienced renal pathological alterations compared with the control group including increased mesangial matrix indicated by hematoxylin and eosin (H&E) staining and obvious segmental glomerulosclerosis indicated by PAS staining. Since the limitations of DN animal models, no interstitial lesions were observed in all DN rats from Masson staining. Overtly, DHQ treatment alleviated the increased renal lesions especially in the groups with DHQ 100 mg/kg/day (Fig. 1G and H). DHQ attenuated renal fibrosis through inhibition of extracellular matrix(ECM) accumulation and mesangial matrix expansion in DN. Furthermore, immunohistochemical staining was conducted to evaluate the expression of IL-1β in each group and found that IL-1β was expressed in normal glomerular tissues and was significantly up-regulated in diabetic nephropathy rats. With the DHQ treatment at the dose of 50 mg/kg/day and 100 mg/kg/day, IL-1β was significantly down-regulated compared to DN group (Fig. S1A and S1B).

Collectively, DHQ exerted kidney protection effects on HFD/STZ -induced DN rats by attenuating the increasing urine microalbumin

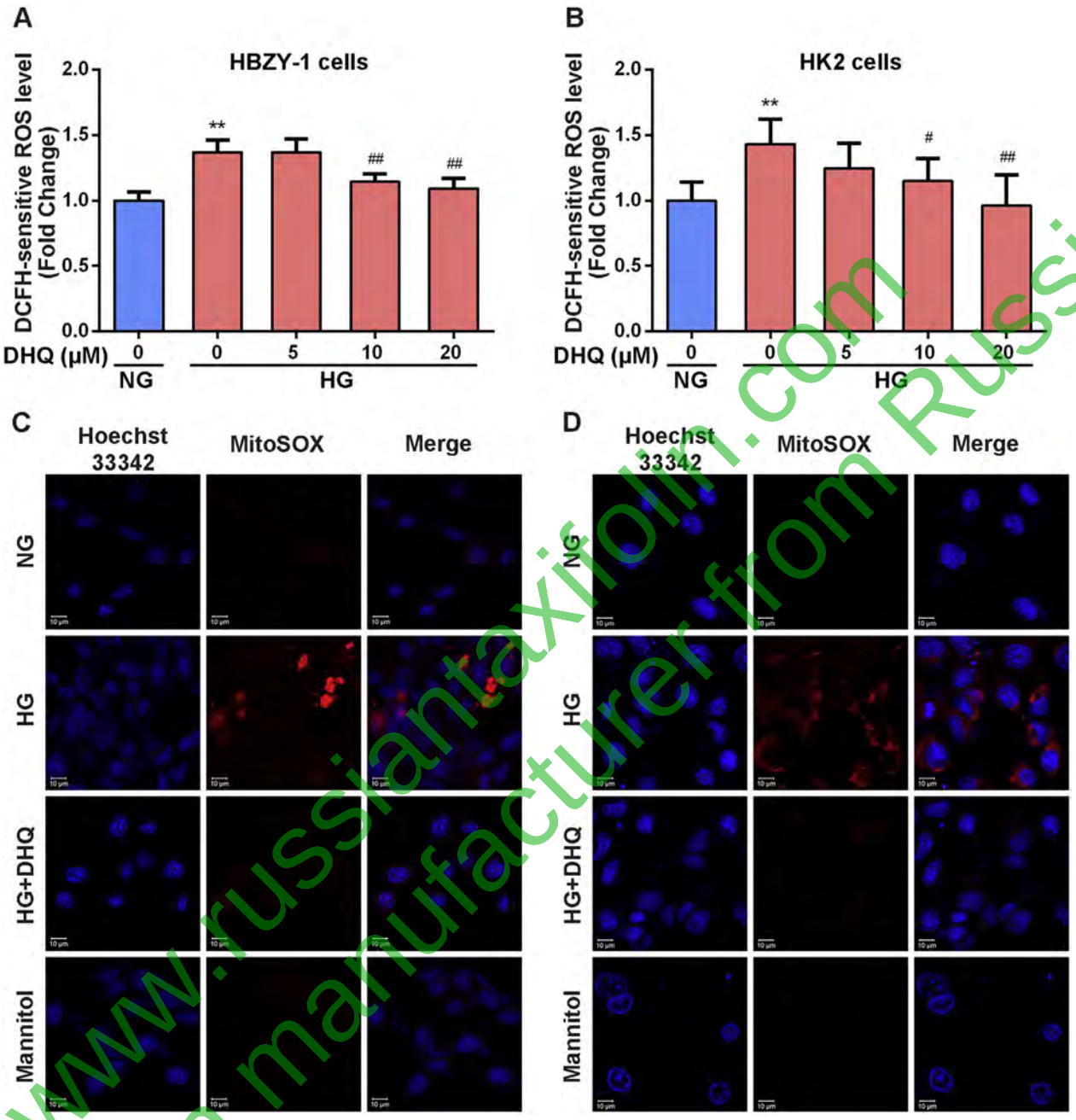

Fig. 3. Effect of DHQ on the intracellular ROS generation and mitochondrial ROS production in HBZY-1 and HK2 cells. (A) and (B) were the intracellular ROS generation determined by DCFH-DA in HBZY-1 cells and HK2 cells respectively. Data were presented by mean ± S.D. $N = 6$ per group ($^{*}P < 0.05$, $^{**}P < 0.01$ versus the NG group; $^{\#}P < 0.05$, $^{\#\#}P < 0.01$ versus the HG group). (C) and (D) were the determination of mitochondrial ROS production measured by confocal microscopy using 100 nM MitoSOX (red) with or without 20 μM DHQ in the presence or absence of high glucose (30 mM) in HBZY-1 cells and HK2 cells respectively. Scale bar = 10 μm. (For interpretation of the references to color in this figure legend, the reader is referred to the web version of this article.)

excretion, hyperglycemia and levels of low density lipoprotein cholesterol and total cholesterol, and mitigating renal histopathological lesions.

Effect of DHQ on the proliferation of HBZY-1 and HK2 cells induced by high glucose

MTT assay was employed to investigate the impact of DHQ on the proliferation of HBZY-1 and HK2 cells. As demonstrated in Fig. 2A, cell proliferation of HBZY-1 increased after 48 h ($P < 0.05$) and 72 h ($P < 0.05$) compared with the normal glucose group when cells exposed to high glucose, and gradually decreased after supplement with DHQ at different concentrations. Specially, cell proliferation of groups with DHQ at the concentration more than 20 μM was significantly lower than those of the HG group after 48 h ($P < 0.05$) and 72 h ($P < 0.01$). As shown in Fig. 2B, cell proliferation of HK2 increased after 48 h ($P < 0.01$) and 72 h ($P < 0.05$) exposure to high glucose compared with the normal glucose group, and decreased significantly in the groups with DHQ at a concentration higher than 20 μM after 48 h ($P < 0.01$) and 72 h ($P < 0.01$) compared with the HG group without DHQ. These results suggested that DHQ significantly suppressed the proliferation of HBZY-1 and HK2 cells induced by high glucose.

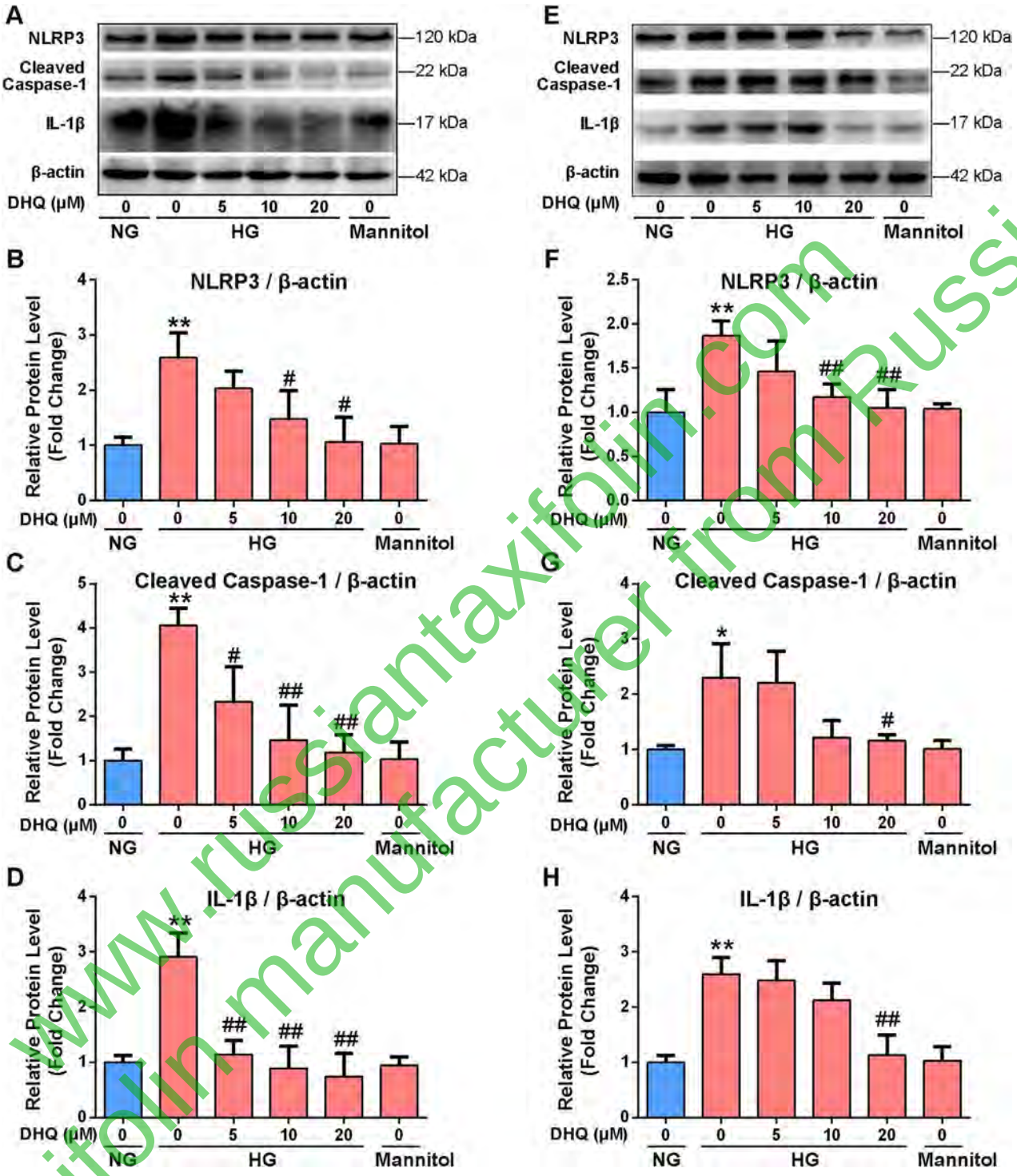

Fig. 4. Effect of DHQ on the activation of NLRP3 inflammasome induced by high glucose in HBZY-1 and HK2 cells. (A) and (E) were the representative western blots for intracellular NLRP3, Cleaved Caspase-1 and IL-1β with β-actin as loading control in HBZY-1 and HK2 cells respectively. (B-D) were the Semi-quantitative analysis of NLRP3, Cleaved Caspase-1 and IL-1β compared with the β-actin in the HBZY-1 cells. (F-H) were the Semi-quantitative analysis of NLRP3, Cleaved Caspase-1 and IL-1β compared with the β-actin in the HK2 cells. Densitometric values were quantified by the ImageJ software, and data represented mean of three independent experiments ($^{*}P < 0.05$, $^{**}P < 0.01$ versus the NG group. $^{\#}P < 0.05$, $^{\#\#}P < 0.01$ versus the HG group).

Effect of DHQ on the intracellular ROS generation and mitochondrial ROS production induced by high glucose in HBZY-1 and HK2 cells

Intracellular and mitochondrial ROS of HBZY-1 and HK2 cells were measured by using DCFH-DA assay and fluorescent probe MitoSOX, respectively. A significant rise in ROS levels was observed for these cells when exposed to the high glucose compared with the normal glucose group, and ROS levels decreased after supplement with DHQ in a concentration-dependent manner. Specially, DHQ at the concentration of 10 μM and 20 μM significantly inhibited the ROS generation in HBZY-1 ($P < 0.01$, $P < 0.01$) (Fig. 3A) and HK2 cells ($P < 0.05$, $P < 0.01$) (Fig. 3B). As shown in Fig. 3C and D, the increased mitochondrial ROS generation observed in the HG group, represented by the red fluorescence, was inhibited by DHQ at the concentration of

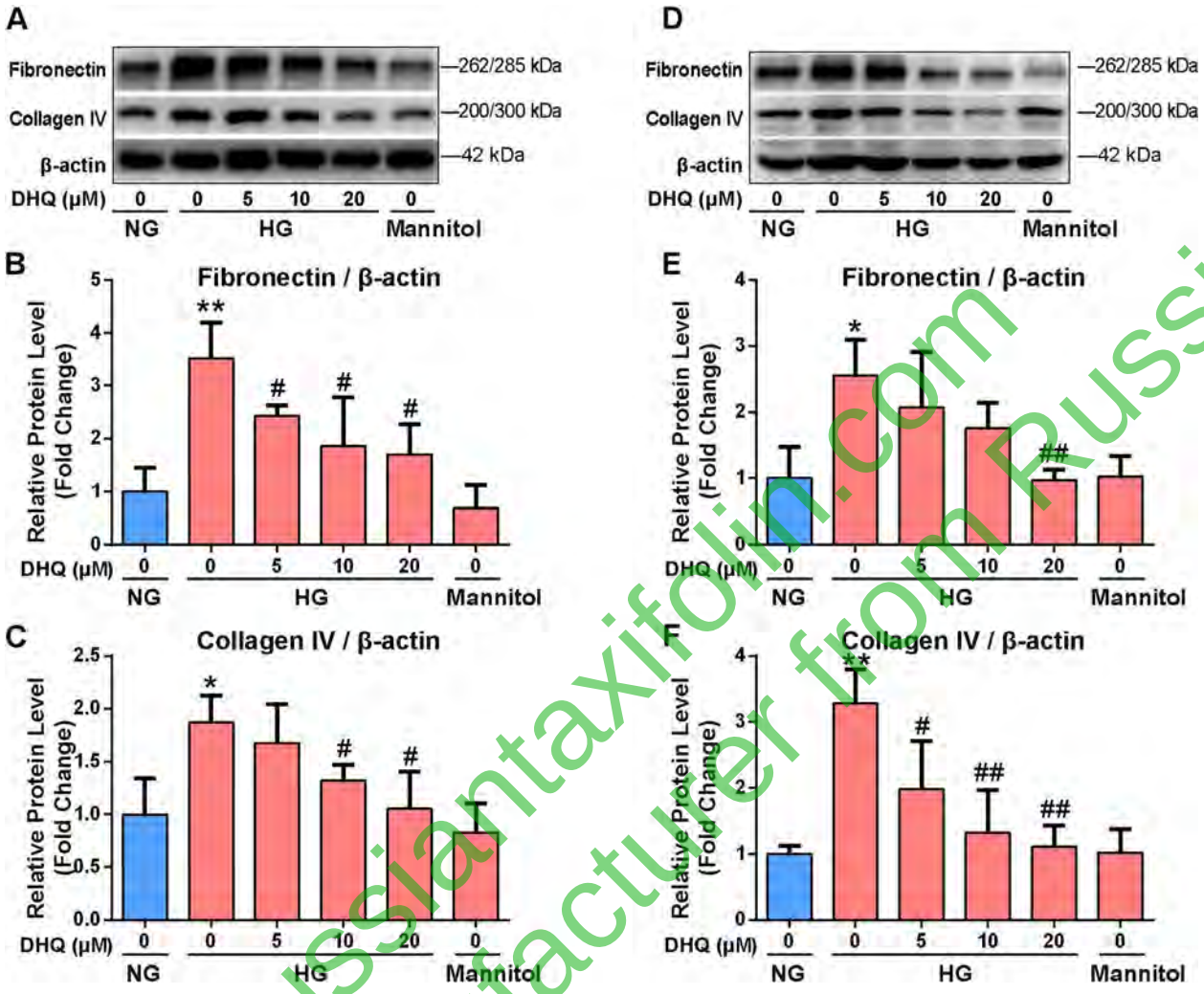

Fig. 5. Effect of DHQ on the expression of protein Fibronectin and Collagen IV induced by high glucose in HBZY-1 and HK2 cells. (A) and (D) were the indicated Western-Blots expression of Fibronectin and Collagen IV in HBZY-1 and HK2 cells respectively. (B) and (C) were the Semi-quantitative analysis of Fibronectin and Collagen IV compared with the β-actin in the HBZY-1 cells. (E) and (F) were the Semi-quantitative analysis of Fibronectin and Collagen IV compared with the β-actin in the HK2 cells. Densitometric values were quantified by the ImageJ software, and data represented mean of three independent experiments ($^{*}P < 0.05$, $^{**}P < 0.01$ versus the NG group. $^{\#}P < 0.05$, $^{\#\#}P < 0.01$ versus the HG group).

20 μM. Moreover, there was no significant difference between the normal glucose group and the mannitol group in the mitochondrial ROS generation. The two ROS detection experiments thus confirmed the antioxidant ability of DHQ in a concentration-dependent manner on the renal cells induced by high glucose. Taken together, DHQ suppressed the intracellular ROS generation and mitochondrial ROS production induced by high glucose in HBZY-1 and HK2 cells.

Effect of DHQ on the activation of NLRP3 inflammasome induced by high glucose in HBZY-1 and HK2 cells

As shown in Fig. 4A, Western-blot of HBZY-1 cell lysates demonstrated that the elevated protein activations of NLRP3, Cleaved Caspase-1 and IL-1β in cells exposed to high glucose were decreased after supplementation with DHQ in HG groups. Especially, semi-quantitative analysis proved that levels of these proteins in the group with DHQ 20 μM were significantly lower than those in the HG group (NLRP3: $P < 0.05$; Cleaved Caspase-1: $P < 0.01$; IL-1β: $P < 0.01$) (Fig. 4B–D). Furthermore, the changes of NLRP3-related proteins appeared in the HK2 cells were similar to the HBZY-1 cells (Fig. 4E), and the semi-quantitative analysis showed that the NLRP3-related proteins were normalized in the group of DHQ 20 μM compared to the NG group and were overtly lower than in the HG group without DHQ (NLRP3: $P < 0.01$; Cleaved Caspase-1: $P < 0.05$; IL-1β: $P < 0.01$) (Fig. 4F–H).

These results demonstrated that DHQ attenuated the activation of NLRP3 inflammasome as well as Cleaved Caspase-1 and IL-1β expression induced by high glucose in HBZY-1 and HK2 cells.

Effect of DHQ on the expressions of renal fibrosis-associated proteins induced by high glucose in HBZY-1 and HK2 cells

As demonstrated in Fig. 5A, the expressions of Fibronectin and Collagen IV in HBZY-1 cells, also known as ECM proteins, increased after exposure to high glucose and gradually decreased after supplement of DHQ. Semi-quantitative analysis of three independent experiments verified the expressions of Fibronectin and Collagen IV in HBZY-1 cells were significantly higher in the HG group than those in the NG group (Fibronectin: $P < 0.01$; Collagen IV: $P < 0.05$) and were significantly lower in groups with DHQ at the concentrations of 10 μM and 20 μM than those in the HG group ($P < 0.05$) (Fig. 5B and C). As shown in Fig. 5D, the change in the expressions of Fibronectin and Collagen IV in HK2 cells was similar to the change in HBZY-1 cells. Semi-quantitative analysis demonstrated that the expressions of Fibronectin and Collagen IV in HK2 cells increased significantly in the HG group compared with those in the NG group (Fibronectin: $P < 0.05$; Collagen IV: $P < 0.01$) and decreased significantly in groups with DHQ at the concentration of 20 μM specially (Fibronectin: $P < 0.01$; Collagen IV: $P < 0.01$) (Fig. 5E and F).

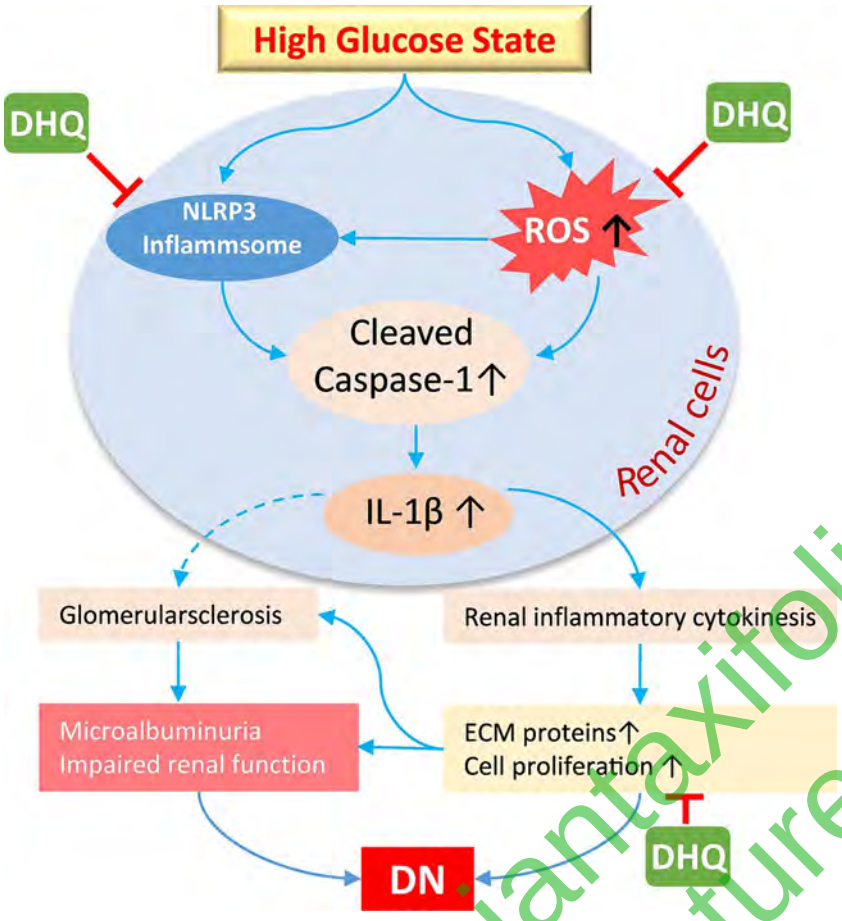

Fig. 6. Overview of potential mechanisms underlying kidney protection effects of DHQ on DN. High glucose state not only promotes generation of ROS and activation of NLRP3 inflammasome, but also stimulates the increased accumulation of ECM proteins in DN which can cause renal glomerulosclerosis. The activation of Cleaved Caspase-1 induced by NLRP3 inflammasome promotes IL-1β secretion followed by renal inflammatory cytokinesis. DHQ could attenuate the progression of DN through suppressing ROS and NLRP3 inflammasome as well as cell proliferation and expressions of ECM proteins.

Taken together, these results suggested that DHQ alleviated the expressions of renal fibrosis-associated proteins including Fibronectin and Collagen IV induced by high glucose in HBZY-1 and HK2 cells.

Discussion

Diabetes results in inflammation, increased adiposity, and chronic hyperglycaemia, and progresses to DN characterized by clinical microalbuminuria and impaired glomerular filtration function. Microalbuminuria resultant from glomerular hyperfiltration in the early stage of DN is an early risk indicator of DN and a predictor of progression as well as a risk factor to cardiovascular disease, and remains the gold standard marker for early diagnosis of DN even though with some limitations (Uwaezuoke, 2017). The characteristic pathological lesion of DN is the accumulated ECM components in glomeruli, mostly resulting in ESRD with development of glomerulosclerosis and loss of renal function although with intensive control of glucose, lipids and blood pressure (Betz and Conway, 2016). We firstly investigated the kidney protection effects and potential mechanisms of DHQ on DN both *in vivo* and *in vitro*. Our results revealed that DHQ significantly attenuated the increasing urine microalbumin excretion, serum level of creatinine, hyperglycemia and lipid metabolism disorders, and mitigated renal histopathological lesions in DN rats through attenuating renal fibrosis via inhibition of ECM accumulation and mesangial matrix expansion in DN, which suggested that DHQ might be a new medicine to treat DN.

It has been generally known that oxidative stress and inflammatory response are interrelated in DN (Sharaf El Din et al., 2016). High glucose not only promotes generation of ROS and activation of NLRP3 inflammasome (Luis-Rodriguez et al., 2012)(Fig. 6), but also stimulates the increased accumulation of ECM proteins including Fibronectin and Collagen IV in DN which can cause renal glomerulosclerosis and tubulointerstitial fibrosis (Wang et al., 2017). ROS generation, among the initial activation and core events of classic DN pathogenesis, can activate inflammatory mediators through the phosphoinositide 3-kinase (PI3K) pathway (Cruz et al., 2007). ATP can produce ROS, which can activate PI3K pathway, thereby promoting Caspase-1 activation and IL-1β secretion in macrophage (Fernandes-Alnemri et al., 2007). The thioredoxin- interacting protein, known as a key regulator of NLRP3 inflammatory mediators induced by hyperglycemia or high glucose state, constitutes a sensor with NLRP3 for cell stress to recognize excessive oxidative stress or dangerous signaling and to trigger inflammatory responses. After ROS stimulation, thioredoxin-interacting protein was released from oxidized thioredoxin and directly binds to the LRR domain of NLRP3 to mediate the assembly of inflammasome (Fitzgerald, 2010). ROS can also cause NF-κB and p38MAPK signaling to activate NLRP3 inflammasome (Bauernfeind et al., 2011). Then the activated NLRP3 inflammasome stimulates the secretion of pro-inflammatory cytokines followed by the Caspase-1 activation and activating chronic low-grade inflammation. Furthermore, ROS accelerates the excessive ECM accumulation by promoting the production of renal inflammatory cytokines.

Therefore, many drugs with antioxidant and anti-inflammatory activities have been investigated to treat and retard DN (Lu et al., 2015), and previous studies have shown that many medicines ameliorated DN through inhibition of NLRP3 inflammasome activation (Lu et al., 2017). However, the connection between DHQ and the NLRP3 inflammasome in DN hasn't been investigated yet. Consistent with these studies about inhibition of NLRP3 inflammasome, our results showed that high glucose stimulation induced cell proliferation, excess ROS generation, activated NLRP3 inflammasome and ECM protein expression in HBZY-1 and HK2 cells. DHQ suppressed the cell proliferation, excess

intracellular and mitochondrial ROS generation induced by high glucose, and significantly decreased the elevated activation of NLRP3 inflammasome as well as the cleaved Caspase-1 and IL-1β expressions induced by high glucose in HBZY-1 and HK2 cells. Furthermore, DHQ attenuated the expression of renal fibrosis-associated proteins Fibronectin and Collagen IV, which reflected the underlying mechanism of the decreased ECM accumulation and mesangial matrix expansion.

As one of the most important microangiopathy of diabetes, DN brings about increasing fractional excretion of calcium, phosphorus, and uric acid when progresses to chronic kidney disease accompanied by a progressive reduction in glomerular filtration (Musso et al., 2012). Recent researches demonstrated that DHQ improved micro-vascularization and microcirculation in the cerebral cortex of SHR rats during the formation of arterial hypertension (Plotnikov et al., 2017), and suppressed uric acid production in plasma and liver via inhibition of hepatic xanthine oxidase activity(Adachi et al., 2017). The combined treatment with a novel agent glucosamine alendronate and DHQ appears to be more effective at maintaining strength of the femur and bone mineral density in OXYS rats of osteoporosis when compared with the monotherapy of glucosamine alendronate (Muraleva et al., 2012). Since animal models always exhibit early lesions of DN, we didn't explore the effects of DHQ on the metabolic disorders of uric acid and calcium which usually appear in advanced DN. There is also a new study bringing a different insight which showed that 11β-hydroxysteroid dehydrogenase 2 (11β-HSD2) which was a mineralocorticoid receptor and primarily expressed in the human and rat kidney, was inhibited by DHQ and then caused the apparent mineralocorticoid excess syndrome with hypertension and hypokalemia (Wu et al., 2017). This might be a side effect in the future research of DHQ when applied to DN. At the current time, there is still much to learn about the effects and mechanisms of DHQ on DN, and further studies will clearly be required to verify these uncertainties.

Conclusion

In conclusion, our study demonstrated that DHQ could attenuate urine microalbumin excretion, serum level of creatinine, hyperglycemia and lipid metabolism disorders, and mitigated renal histopathological lesions in DN rats. Furthermore, the underlying mechanisms of the renal protective effects of DHQ were preliminarily verified through suppressing the ROS generation, alleviating the activation of NLRP3 inflammasome and the expression of renal fibrosis-associated proteins. Taken together, these results suggested that DHQ exerted kidney protection effects on DN through suppressing the ROS and activation of NLRP3 inflammasome.

Acknowledgments

This work was supported by grants from the National Natural Science Foundation of China (81773620 and 81573332), National Key Basic Research Program of China (2015CB931800), the Scientific Research Projects of Shanghai Municipal Commission of Health and Family Planning (201740140), and the Research and Innovation Projects of Shanghai Municipal Education Commission (13ZZ063).

Conflict of interest

The authors declare no conflict of interest.

Supplementary materials

Supplementary material associated with this article can be found, in the online version, at doi:10.1016/j.phymed.2018.01.026.

References

Adachi, S.I., Nihei, K.I., Ishihara, Y., Yoshizawa, F., Yagasaki, K., 2017. Anti-hyperuricemic effect of taxifolin in cultured hepatocytes and model mice. Cytotechnology 69, 329–336.
Bauernfeind, F., Bartok, E., Rieger, A., Franchi, L., Nunez, G., Hornung, V., 2011. Cutting edge: reactive oxygen species inhibitors block priming, but not activation, of the NLRP3 inflammasome. J. Immunol. 187, 613–617.
Betz, B., Conway, B.R., 2016. An update on the use of animal models in diabetic nephropathy research. Curr. Diab. Rep. 16, 18.
Casaschi, A., Rubio, B.K., Maiyoh, G.K., Theriault, A.G., 2004. Inhibitory activity of diacylglycerol acyltransferase (DGAT) and microsomal triglyceride transfer protein (MTP) by the flavonoid, taxifolin, in HepG2 cells: potential role in the regulation of apolipoprotein B secretion. Atherosclerosis 176, 247–253.
Cruz, C.M., Rinna, A., Forman, H.J., Ventura, A.L., Persechini, P.M., Ojcius, D.M., 2007. ATP activates a reactive oxygen species-dependent oxidative stress response and secretion of proinflammatory cytokines in macrophages. J. Biol. Chem. 282, 2871–2879.
Elmarakby, A.A., Sullivan, J.C., 2012. Relationship between oxidative stress and inflammatory cytokines in diabetic nephropathy. Cardiovasc. Ther. 30, 49–59.
Fernandes-Alnemri, T., Wu, J., Yu, J.W., Datta, P., Miller, B., Jankowski, W., Rosenberg, S., Zhang, J., Alnemri, E.S., 2007. The pyroptosome: a supramolecular assembly of ASC dimers mediating inflammatory cell death via caspase-1 activation. Cell Death Differ. 14, 1590–1604.
Fitzgerald, K.A., 2010. NLR-containing inflammasomes: central mediators of host defense and inflammation. Eur. J. Immunol. 40, 595–598.
Guo, H., Zhang, X., Cui, Y., Zhou, H., Xu, D., Shan, T., Zhang, F., Guo, Y., Chen, Y., Wu, D., 2015. Taxifolin protects against cardiac hypertrophy and fibrosis during biomechanical stress of pressure overload. Toxicol. Appl. Pharmacol. 287, 168–177.
Lopes, A.A., 2009. End-stage renal disease due to diabetes in racial/ethnic minorities and disadvantaged populations. Ethn. Dis. 19 S1-47-51.
Lu, M., Yin, N., Liu, W., Cui, X., Chen, S., Wang, E., 2017. Curcumin ameliorates diabetic nephropathy by suppressing NLRP3 inflammasome signaling. BioMed Res. Int. 2017, 1516985.
Lu, Q., Zuo, W.Z., Ji, X.J., Zhou, Y.X., Liu, Y.Q., Yao, X.Q., Zhou, X.Y., Liu, Y.W., Zhang, F., Yin, X.X., 2015. Ethanolic *Ginkgo biloba* leaf extract prevents renal fibrosis through Akt/mTOR signaling in diabetic nephropathy. Phytomedicine 22, 1071–1078.
Luis-Rodriguez, D., Martinez-Castelao, A., Gorriz, J.L., De-Alvaro, F., Navarro-Gonzalez, J.F., 2012. Pathophysiological role and therapeutic implications of inflammation in diabetic nephropathy. World J. Diabetes 3, 7–18.
Maksimovich, N.Y., Dremza, I.K., Troian, E.I., Maksimovich, Y.N., Borodinskii, A.N., 2014. The correcting effects of dihydroquercetin in cerebral ischemia-reperfusion injury. Biomed. Khim. 60, 643–650.
Muraleva, N.A., Ofitserov, E.N., Tikhonov, V.P., Kolosova, N.G., 2012. Efficacy of glucosamine alendronate alone and in combination with dihydroquercetin for treatment of osteoporosis in animal model. Indian J. Med. Res. 135, 221–227.
Musso, C.G., Juarez, R., Vilas, M., Navarro, M., Rivera, H., Jauregui, R., 2012. Renal calcium, phosphorus, magnesium and uric acid handling: comparison between stage III chronic kidney disease patients and healthy oldest old. Int. Urol. Nephrol. 44, 1559–1562.
Nankar, R.P., Doble, M., 2017. Hybrid drug combination: anti-diabetic treatment of type 2 diabetic Wistar rats with combination of ellagic acid and pioglitazone. Phytomedicine 37, 4–9.
Plotnikov, M.B., Aliev, O.I., Sidekhmenova, A.V., Shamanaev, A.Y., Anishchenko, A.M., Fomina, T.I., Chernysheva, G.A., Smol'yakova, V.I., Arkhipov, A.M., 2017. Dihydroquercetin improves microvascularization and microcirculation in the brain cortex of SHR rats during the development of arterial hypertension. Bull. Exp. Biol. Med. 163, 57–60.
Sharaf El Din, U.A., Salem, M.M., Abdulazim, D.O., 2016. Stop chronic kidney disease progression: time is approaching. World J. Nephrol. 5, 258–273.
Si, X., Li, P., Zhang, Y., Zhang, Y., Lv, W., Qi, D., 2014. Renoprotective effects of olmesartan medoxomil on diabetic nephropathy in streptozotocin-induced diabetes in rats. Biomed Rep. 2, 24–28.
Sun, X., Chen, R.C., Yang, Z.H., Sun, G.B., Wang, M., Ma, X.J., Yang, L.J., Sun, X.B., 2014. Taxifolin prevents diabetic cardiomyopathy *in vivo* and *in vitro* by inhibition of oxidative stress and cell apoptosis. Food Chem. Toxicol. 63, 221–232.
Uwaezuoke, S.N., 2017. The role of novel biomarkers in predicting diabetic nephropathy: a review. Int. J. Nephrol. Renovasc. Dis. 10, 221–231.
Vega-Diaz, N., Gonzalez-Cabrera, F., Marrero-Robayna, S., Santana-Estupinan, R., Gallego-Samper, R., Henriquez-Palop, F., Perez-Borges, P., Rodriguez-Perez, J.C., 2015. Renal replacement therapy: Purifying efficiency of automated peritoneal dialysis in diabetic versus non-diabetic patients. J. Clin. Med. 4, 1518–1535.
Vladimirov, Y.A., Proskurnina, E.V., Demin, E.M., Matveeva, N.S., Lubitskiy, O.B., Novikov, A.A., Izmailov, D.Y., Osipov, A.N., Tikhonov, V.P., Kagan, V.E., 2009. Dihydroquercetin (taxifolin) and other flavonoids as inhibitors of free radical formation at key stages of apoptosis. Biochemistry 74, 301–307.
Wang, S., Zhao, X., Yang, S., Chen, B., Shi, J., 2017. Salidroside alleviates high glucose-induced oxidative stress and extracellular matrix accumulation in rat glomerular mesangial cells by the TXNIP-NLRP3 inflammasome pathway. Chem. Biol. Interact. 278, 48–53.
Weidmann, A.E., 2012. Dihydroquercetin: More than just an impurity? Eur. J. Pharmacol. 684, 19–26.
Wu, C., Cao, S., Hong, T., Dong, Y., Li, C., Wang, Q., Sun, J., Ge, R.S., 2017. Taxifolin inhibits rat and human 11-beta-hydroxysteroid dehydrogenase 2. Fitoterapia 121, 112–117.
Yang, P., Xu, F., Li, H.F., Wang, Y., Li, F.C., Shang, M.Y., Liu, G.X., Wang, X., Cai, S.Q., 2016. Detection of 191 taxifolin metabolites and their distribution in rats using HPLC-ESI-IT-TOF-MSn. Molecules 21, 1209.
Zheng, S., Powell, D.W., Zheng, F., Kantharidis, P., Gnudi, L., 2016. Diabetic nephropathy: proteinuria, inflammation, and fibrosis. J Diabetes Res. 2016, 5241549.